

RSC Advances



This is an *Accepted Manuscript*, which has been through the Royal Society of Chemistry peer review process and has been accepted for publication.

Accepted Manuscripts are published online shortly after acceptance, before technical editing, formatting and proof reading. Using this free service, authors can make their results available to the community, in citable form, before we publish the edited article. This *Accepted Manuscript* will be replaced by the edited, formatted and paginated article as soon as this is available.

You can find more information about *Accepted Manuscripts* in the [Information for Authors](#).

Please note that technical editing may introduce minor changes to the text and/or graphics, which may alter content. The journal's standard [Terms & Conditions](#) and the [Ethical guidelines](#) still apply. In no event shall the Royal Society of Chemistry be held responsible for any errors or omissions in this *Accepted Manuscript* or any consequences arising from the use of any information it contains.

Influence of matrix modulus on the mechanical and interfacial properties of carbon fiber filament wound composites

Qingjie Zhang,^a Shengbiao Liang,^a Gang Sui^{*a} and Xiaoping Yang^a

The effect of epoxy resin matrix modulus on the mechanical and interfacial properties of T700 carbon fiber and T800 carbon fiber filament wound composites was investigated. Different aromatic amine curing agents were selected to change the modulus of the same kind of resin matrix. The mechanical properties of carbon fiber filament wound composites were characterized through Naval Ordnance Laboratory-ring (NOL) burst tests, and interlaminar shear strength (ILSS) tests. Scanning electron microscopy (SEM), atomic force microscopy (AFM) and dynamic mechanical thermal analysis (DMA) were used to characterize the failure surfaces and interfacial properties of the resulting composites. The results showed that, even if carbon fibers were fully impregnated with epoxy resin, the mechanical properties of composites and the mode of interfacial failure were closely related to the modulus of resin matrix. The resin matrix with high modulus was found to be an essential prerequisite to excellent mechanical and interfacial properties of the resulting composites.

Introduction

Carbon fiber reinforced polymer composites (CFRP) has been aroused considerable scientific and industrial attention because of their attractive mechanical properties such as high specific stiffness and high strength, as well as a relatively high tolerance of environmental changes¹. At present, the filament winding applications for these composites are the pressure vessels, pipes and shafts². A good design that exploits the desired strength and toughness of the fiber reinforced composites requires a basic understanding: (1) the significance of the fiber, epoxy matrix and fiber-matrix interfacial region in composites; and (2) the relationship between the structure, deformation and failure processes and mechanical response of the fiber, epoxy matrix and their interface.

The interface is a complicated phase, which is different from reinforcements and resin matrix³. Good interfacial properties can improve integral mechanical properties of fiber-reinforced composites via reducing stress concentrations caused by load transfer from matrix to reinforcements⁴. In order to improve the interfacial properties of CFRP, scientific efforts have been devoted to treat carbon fibers by a variety of methods such as electrochemically treatment⁵, plasma oxidation^{6, 7}, sizing modification⁸⁻¹⁰. However, according to the existing the rational allocation researches, matrix is still the main factor to control the load transfer in composites^{11, 12} which determines the interfacial and the mechanical properties of composites.

In our previously works, we proved that the chemical reaction of carbon fiber/epoxy system was epoxy-amine reactions in two interphases to form a three-dimensional network. And, we also found that the strong polar tertiary amine groups in amine-cured epoxy matrix would possess good interfacial adhesion with carbon fibers¹². Though good interfacial adhesion with carbon fibers has been obtained, the in-depth study on the relationship between the modulus of resin matrix and mechanical and interfacial properties of carbon fiber/epoxy composites is still to be needed.

The major objective of this work is to investigate the effect of resin matrix modulus on the mechanical and interfacial properties of carbon fiber/epoxy composites. Special emphasis is placed on the rational adjustment of the hardeners, for constructing the matrix with different modulus. And the processing carbon fiber/epoxy composites were carried out by the wet filament winding. Meanwhile, the mechanical properties of the resulting composites were

characterized through Naval Ordinance Laboratory-ring (NOL) burst tests, and interlaminar shear strength (ILSS) tests. In order to relate the interface behavior with the characteristics of the matrix, several techniques, such as scanning electron microscopy (SEM), atomic force microscopy (AFM) and dynamic mechanical thermal analysis (DMA) had been used to characterize the interfacial properties of composites.

Experiment

Material

DGEAC is diglycidyl ester of aliphatic cycle type epoxy resin which was supplied by Tianjin jindong chemical industrial factory (epoxy value, 0.85). 4, 4'-Diaminodiphenyl methane (DDM) were supplied by Tianjin Synthetic Material Research Institute, China. A mixture of the two diethyltoluene diamine (DETDA) isomers (74–80% 2, 4-isomer and 18–24% 2, 6-isomer) was supplied by Ethacure 100 of Albemarle Corp, USA. 4, 4'-Diamino diphenyl sulone (DDS) were supplied form Suzhou Yinsheng chemical company. The chemical structures of the resins and hardeners are shown in Table 1. The liquid aromatic diamine (DETDA) was selected to use with DDM or DDS, because of its less reactivity¹³. Therefore, the modified hardeners, which was the mixture of the DDM (or DDS) and DETDA in special ratio, possesses low melting point and proper reactivity. The ratio of epoxy/amine in each system was equivalent stoichiometric to form completely cured epoxide-amine cross-linking networks¹⁴.

T700 and T800 carbon fibers were obtained from Toray Company. The surface morphologies are shown in Fig.1 and properties of carbon fiber are listed in Table 2. T800 carbon fiber shows clear trench structure along the axes of fiber which could obtain better interface performance¹² of the resulting composites than T700 ones via improving the contact area of between fiber and matrix and impregnation of resin matrix. All of these materials utilized in this experiment without further purification.

Composites preparation

For the resin casts and the resulting carbon fiber composites, the curing condition “80°C/1h+120°C/2h+150°C/3h+180°C/1h” was used when the hardener was DDM. Meanwhile the curing condition “80°C/1h+120°C/2h+150°C/3h+180°C/2h” was used when the hardener

was DDM /DETDA, and “80°C/1h+120°C/2h+150°C/3h+180°C/3h” was used when the hardener was DETDA or DDS/DETDA”. NOL ring is one kind of CFRP composites which is produced by filament winding. Not only can it reflect the capability of the composites to transfer the load, but also can be used to assess the interfacial adhesion of the composites^{12,15}. In this work, NOL rings were produced by a filament winding machine (MAW20-LS1-6, Mikrosam Company, Macedonia) with 25N Winding tension. Unidirectional carbon fiber/epoxy composites were prepared by manual winding on unidirectional mould, then placed in oven and cured. The fiber volume fraction of NOL rings and unidirectional carbon fiber/epoxy composites were controlled at 60%.

Analysis and characterization

According ASTM D 638, the tensile performance of resin casts were tested on Instron-1121 universal testing machine with testing speed at 2 mm/min. Six specimens were measured for every case and the average values were taken.

The details of the NOL test specimen specifications are provided in Fig. 2. According to ASTM D 2290-00, the tensile strength of the NOL ring was tested on an INSTRON-1196 universal testing machine at a rate of 5 mm/min. It should be noted that the tensile strength, σ as characterized by the NOL ring burst test can be determined as

$$\sigma = \frac{P}{2t\omega} \quad (1)$$

where P is the ultimate burst force recorded, t and w is the thickness and width of the NOL ring respectively. Six specimens were measured for every case and the average values were taken.

According to ASTM D 2344, ILSS of unidirectional composites was carried out on INSTRON-1196 universal testing machine with testing speed at 2 mm/min. The composites were machined along the fiber direction into 20 mm×6 mm short-beam-shear specimens with 2 mm thickness. Tests were also conducted at 6/1 span-to depth ratio. Six specimens were measured for every case and the average values were taken.

The fracture surfaces of the epoxy and the resulting carbon fiber reinforced composites were observed with SEM (4700S, HITACHI Co., Japan). All samples were sputter-coated with gold to avoid the electric charge.

The surface roughness of the carbon fiber composites was measured with AFM

(Nanoscope IIIa, Digital Instrument Co., USA) by fastening a carbon fiber filament to a steel sample mount using double sided tape with a scanning region of 2 μm ×2 μm . NanoScope Analysis software was used to calculate the roughness R_a and R_{max} , where R_a is the arithmetic average of the absolute values of the surface height deviations and R_{max} is the difference in height between the highest and lowest points on the cross-sectional profile relative to the center line over the length of the profile¹⁶, and at least 20 valid data were applied for each specimen. R_a can be determined by equation (2) as follow:

$$R_a = \frac{1}{n} \sum_{i=1}^n |y_i| \quad (2)$$

where n is the number of sampling points and y_i is the vertical lift of the sampling points. All images were collected in air using the tapping mode with a silicon nitride probe.

The thermal-mechanical property of the samples was measured by DMA (Q800, TA Co. USA) under nitrogen atmosphere with a heating rate of 5 °C/min. The heating temperature ranges from 40 °C to 250 °C, and a constant frequency of 1 Hz was used.

Results and discussion

Mechanical properties and fractography of resin matrix

Three kinds of amine were used as the hardeners of DGEAC in this work. The mechanical properties of resin casts are shown in Table 3. From the Table 3, the resin with the mixed amines showed the higher tensile strength, break elongation and modulus. The highest tensile strength and break elongation were obtained by using DDM/DETDA curing system. The modulus of resin casts was between 2.4 GPa (DGEAC/DDM) and 3.7 GPa (DGEAC/DDS/DETDA). DGEAC/DETDA material system had the same tensile modulus as DGEAC/DDM/DETDA system but much less break elongation than the latter.

SEM micrographs of fractured surfaces of epoxy resins after tensile test are shown in Fig.3. The fracture surface of DGEAC/DETDA showed typical characteristics of brittle fracture (see Fig.3 (b)). The fracture surfaces of other hardener cured epoxy resins were relatively rough. Tortuous cracks, ridges and river marks can be seen on the fracture surfaces (see Fig.3 (a), (c) and (d)). The rough fracture surface indicates deflection of crack path, the crack deviation from its original plane, and increasing the area of the crack. Hence, the required energy for the propagation of the cracks on the fracture surfaces is increased¹⁷. Further, the morphology of the microscopic fracture surfaces showed that all compositions

investigated were homogeneous with no sign of phase separation, suggesting the uniformity of microstructure in all resin systems.

Mechanical and interfacial properties of carbon fiber composites

The tensile strength of NOL-ring composites and ILSS of unidirectional composites are given in Table 4. For T700 carbon fiber, the resulting composites showed the lower tensile strength and ILSS than that of T800 carbon fiber. The main reason is that T800 carbon fibers have more obvious grooved surface microstructure as shown in Fig.1. In addition, the mechanical properties of composites were better if the mixed amines-cured DGEAC were used as matrix. The lowest tensile strength and ILSS of carbon fiber composites were obtained if DGEAC/DDM material system was involved, while the highest properties appeared by adopting DGEAC/DDS/DETDA system. Combining the data of Table 3 and Table 4, there is a good relationship between the modulus of resin matrix and mechanical properties of carbon fiber/epoxy composites. The results show that the resin matrix with high modulus is an essential prerequisite to excellent mechanical properties of the resulting composites.

As shown in Fig.4, the fracture surface of T700 carbon fiber and T800 carbon fiber NOL-ring composites were observed after tensile testing under SEM. The fracture surface of DGEAC/DDS/DETDA samples was uniform and smooth, and carbon fibers were tightly bonded to resin matrix together. Compared to DGEAC/DDS/DETDA samples, DGEAC/DETDA and DGEAC/DDM/DETDA samples, which had moderate modulus, showed slight debonding phenomenon. In contrast, the debonding phenomenon was obvious in DGEAC/DDM samples. Furthermore, the same changed trend of interfacial adhesion was also observed by the fracture surface of T700 carbon fiber and T800 carbon fiber unidirectional composites after ILSS testing under SEM (as shown in Fig.5). With the improvement of modulus of matrix, the resulting carbon fiber composites had stronger interfacial adhesion, with carbon fibers well covered by epoxy matrices. The results show that high matrix modulus could provide better interfacial adhesion properties.

Fig. 6 shows the three-dimensional AFM topographical images of T700 carbon fiber and T800 carbon fiber in composites after failure. Table 5 summarizes the results of the roughness analysis of the resulting composites as obtained from AFM. From Fig. 6, the surface of the

fiber was relatively smooth and only some tiny pieces of resin were residual for the composite matrix with low modulus after tensile failure; with the increase of resin modulus, the resin pieces were connected into a continuous phase which made the surface of carbon fiber have a roughly waved shape. The results show that the mode of interfacial failure varies corresponding to the different modulus of matrix.

The interfacial property between matrix and carbon fiber can also be analyzed through DMTA data by using Luis Ibrarra's empirical equation (3)¹⁸ or Ashida's empirical equation (4)¹⁹:

$$A = \frac{1}{1-V_f} \times \frac{(\tan \delta_{\max})_c}{(\tan \delta_{\max})_m} - 1 \quad (3)$$

$$\alpha = \frac{(\tan \delta_{\max})_m - (\tan \delta_{\max})_c}{V_f} \quad (4)$$

where V_f is the volume fraction of carbon fiber, $(\tan \delta_{\max})_c$ is the largest loss factor of CFRP, and $(\tan \delta_{\max})_m$ is the largest loss factor of matrix. If matrix has a stronger adhesion with carbon fiber, there will be a less value of A or a larger value of α .

Tan δ thermographs of matrices and those of their composites are respectively shown as Fig.7. For each resin matrix, $(\tan \delta_{\max})_m$ appeared at its glass transition temperature (Tg) and a higher Tg can be observed in the carbon fiber composites. It is because that the chain segments movement of matrix has been limited by adhesion between matrix and fiber. In our investigation, V_f is 0.6. Then, interfacial adhesion parameters of the resulting composites can be calculated and summarized in Table 6.

From Table 6, it can be seen that carbon fiber composites displayed the least value of A and largest value of α when matrix was DGEAC/DDS/DETDA system. Therefore, a desirable interfacial property can be realized when the DGEAC/DDS/DETDA system was involved into the composites. Contrarily, the undesired interfacial adhesion appeared in DGEAC/DDM samples.

According to the reference²⁰, the modulus of interface is between that of fibers and matrix. The stress would be concentrated in the interphase and cracks would spread easily along the axis of fiber if the modulus of matrix is low. The failure modes of the composites

are the debonding of fiber-matrix interface. If the modulus of matrix is enhanced, the stress can be fully transferred at the interface between matrix and fiber, and the fracture energy would be absorbed and dissipated along with the propagation of crack. The energy for material failure would be increased and the failure modes of the composites are accompanied by a large amount of matrix damage. The schematic view of the failure modes detected with increasing modulus of matrix under shear stress is shown in Fig.8. Combined with above analyses, it can be substantiated that a high modulus of matrix is beneficial to good interfacial properties of the composites. This result is in good agreement with the mechanical properties of tensile strength of NOL-ring and ILSS of composites.

Conclusions

Through the use of several kinds of amine curing agents, different modulus of DGEAC resin system were obtained. Tensile strength of NOL-ring and ILSS of T700 and T800 carbon fiber reinforced these matrices revealed a noticeable correlativity between mechanical properties of the composites and the modulus of matrix. To take full advantage of the high performance of carbon fiber, high modulus of matrix is an important requirement. The analyses of transverse fracture surface and fiber surface also show that high modulus of matrix is a primary prerequisite to good interfacial properties of the carbon fiber filament wound composites.

Acknowledgments

The authors acknowledge the financial support from the Program for New Century Excellent Talents in University (No. NCET-12-0761) and the National High-tech R&D Program of China (863 Program) (No. 2012AA03A203).

Notes and references

^a State Key Laboratory of Organic-Inorganic Composites, Beijing University of Chemical Technology, Beijing 100029, China

* Corresponding author: Email: suigang@mail.buct.edu.cn; Tel: (86) 10-64427698; Fax: (86) 10-64412084.

- 1 Lee DG, Lee CS, Lee HG, Hwang HY, Kim JW. Novel applications of composite structures to robots, machine tools and automobiles. *Composite Structures*, 2004, 66, 17-39
- 2 Cohen D, Mantell SC, Zhao LY. The effect of fiber volume fraction on filament wound composite pressure vessel strength. *Composites Part B: Engineering*, 2001, 31, 413-429
- 3 Sharma M, Gao SL, Mäder E, Sharma H, Wei LY, Jayashree B. Carbon fiber surfaces and composite interphases. *Composites Science and Technology*, 2004, 102, 35-50
- 4 He HW, Wang JL, Li KX, Wang J, Gu JY. Mixed resin and carbon fibres surface treatment for preparation of carbon fibers composites with good interfacial bonding strength. *Materials and Design*, 2010, 31,4631-4637
- 5 Pittman JC, Jiang W, Yue ZR, et al. Surface properties of electrochemically oxidized carbon fiber. *Carbon*, 1999, 37, 1797-1807
- 6 Montes-Morán MA, Matínez-Alonso A, Tascón JMD, et al. Effect of plasma oxidation on the surface and interfacial properties of carbon fiber/polycarbonate composites. *Carbon*, 2001, 39, 1057-1068.
- 7 Montes-Moran M, Young R. Raman spectroscopy study of high-modulus carbon fibers: effect of plasma-treatment on the interfacial properties of single-fiber-epoxy composite, part I: characterization of the fiber-matrix interface. *Carbon*, 2002, 40, 857-875.
- 8 Zhang RL, Huang YD, Liu L, Tang YR, Su D, Xu LW. Influence of sizing emulsifier content on the properties of carbon fibers and its composites. *Materials and Design*, 2012, 33, 367-371
- 9 Zhang RL, Huang YD, Li N, Liu L, Su D. Effect of the concentration of the sizing agent on the carbon fibers surface and interface properties of its composites. *Journal of Applied Polymer Science*, 2012, 125, 425-432
- 10 Yao LR, Li M, Wu Q, Dai ZS, Gu YZ, Li YX, Zhang ZG. Comparison of sizing effect of T700 grade carbon fiber on interfacial properties of fiber/BMI and fiber/epoxy. *Applied Surface Science*, 2012, 263, 326-333

- 11 Bazhenov SL, Kuperman AM, Zelenskii ES, et al. Compression failure of unidirectional glass fiber reinforced plastics. *Composites Science and Technology*, 1992, 45, 201-208
- 12 Chen WM, Yu YH, Li P, Yang XP. Effect of new epoxy matrix for T800 carbon fiber/epoxy filament wound composites. *Composite Science and technology*, 2007, 67, 2261-2270
- 13 Naffakh M, Dumon M, Dupuy J, Ge´rard JF. Cure kinetics of an epoxy/liquid aromatic diamine modified with poly(etherimide). *Journal of Applied Polymer Science*, 2005, 96, 660-72.
- 14 Dušek K, Dušková-Smrčková M. Network structure formation during cross-linking of organic coating systems. *Progress in polymer science*, 2000, 25, 1215-1260
- 15 Zhang S, Karbharia V.M, Reynaud D. NOL-ring based evaluation of freeze and freeze–thaw exposure effects on FRP composite column wrap systems. *Composites Part B: Engineering*, 2001, 32, 589-598
- 16 Gao SL, McEder E, Zhandarov SF. Carbon fibers and composites with epoxy resins: Topography, fractography and interphases. *Carbon*, 2004, 42, 515-529
- 17 Haris A, Adachi T, Araki W. Nano-scale characterization of fracture surfaces of blended epoxy resins related to fracture properties. *Materials Science and Engineering A*, 2008, 496, 337-344
- 18 Ibrarra L, Panos D. Dynamic properties of thermoplastics butadiene-styrene (SBS) and oxidized short carbon fiber composite materials. *Journal of Applied Polymer Science*, 1998, 67, 1819-1826
- 19 Ashida M, Noguchi T. Effect of matrix’s type on the dynamic properties for short fiber-slastomer composite. *Journal of Applied Polymer Science*, 1985, 30, 1011-1021
- 20 Qi GC, Du SY, Zhang B, Tang ZW, Yu YL. Evaluation of carbon fiber/epoxy interfacial strength in transverse fiber bundle composite: Experiment and multiscale failure modeling. *Composites Science and Technology*, 2014, 105, 1-8

Figure captions

Figure 1—SEM photograph of commercial carbon fibers: (a) T700 carbon fiber and (b) T800 carbon fiber

Figure 2—Details of NOL ring specimens.

Figure 3—Fractographs of epoxy resins: (a) DGEAC/DDM, (b) DGEAC/DETDA, (c) DGEAC/DDM/DETDA and (d) DGEAC/DDS/DETDA

Figure 4—SEM photographs of carbon fiber composites surface after tensile failure: (a) DGEAC/DDM/T700 carbon fiber, (b) DGEAC/DETDA/T700 carbon fiber, (c) DGEAC/DDM/DETDA/T700 carbon fiber, (d) DGEAC/DDS/DETDA/T700 carbon fiber, (e) DGEAC/DDM/T800 carbon fiber, (f) DGEAC/DETDA/T800 carbon fiber, (g) DGEAC/DDM/DETDA/T800 carbon fiber and (h) DGEAC/DDS/DETDA/T800 carbon fiber

Figure 5—SEM photographs of carbon fiber composites surface after ILSS failure: (a) DGEAC/DDM/T700 carbon fiber, (b) DGEAC/DETDA/T700 carbon fiber, (c) DGEAC/DDM/DETDA/T700 carbon fiber, (d) DGEAC/DDS/DETDA/T700 carbon fiber, (e) DGEAC/DDM/T800 carbon fiber, (f) DGEAC/DETDA/T800 carbon fiber, (g) DGEAC/DDM/DETDA/T800 carbon fiber and (h) DGEAC/DDS/DETDA/T800 carbon fiber

Figure 6—Three-dimensional AFM topographical images of T700 carbon fiber and T800 carbon fiber in composites after failure: (a) DGEAC/DDM/T700 carbon fiber, (b) DGEAC/DETDA/T700 carbon fiber, (c) DGEAC/DDM/DETDA/T700 carbon fiber, (d) DGEAC/DDS/DETDA/T700 carbon fiber, (e) DGEAC/DDM/T800 carbon fiber, (f) DGEAC/DETDA/T800 carbon fiber, (g) DGEAC/DDM/DETDA/T800 carbon fiber and (h) DGEAC/DDS/DETDA/T800 carbon fiber

Figure 7—Tan δ thermographs of (a) epoxy matrix, (b) T700 carbon fiber composites and (c) T800 carbon fiber composites

Figure 8—Schematic view of the failure modes detected with increasing modulus of matrix under shear stress

Table captions

Table 1—Chemical structure of materials

Table 2—Properties of the T700 carbon fiber and T800 carbon fiber

Table 3—Mechanical properties of resin casts

Table 4—Mechanical properties of composites

Table 5—Main roughness parameters of carbon fiber in composites after failure by AFM

Table 6—Interfacial adhesion parameters of T700 and T800 carbon fiber/epoxy composites

Figure 1

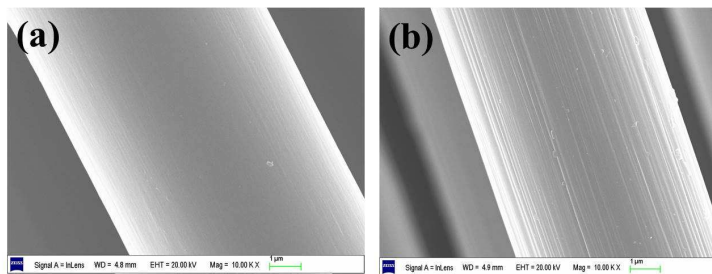


Figure 2

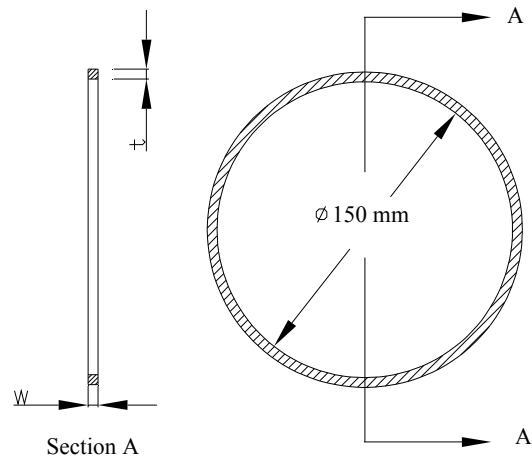


Figure 3

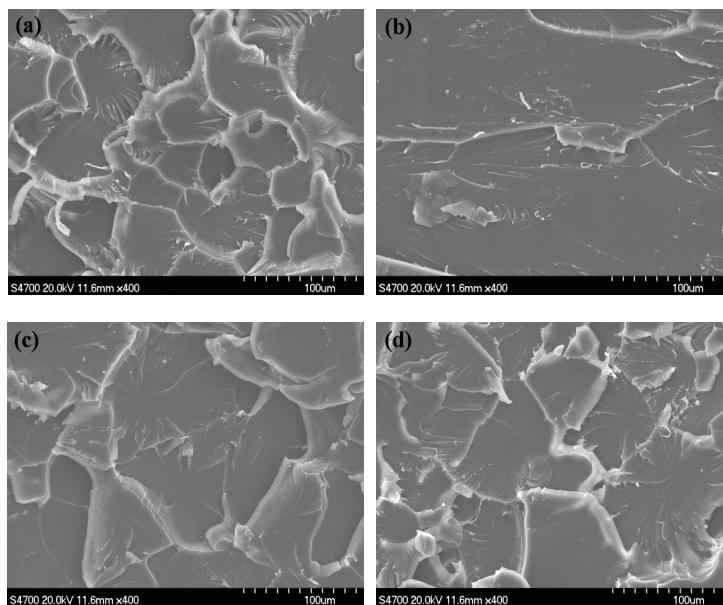


Figure 4

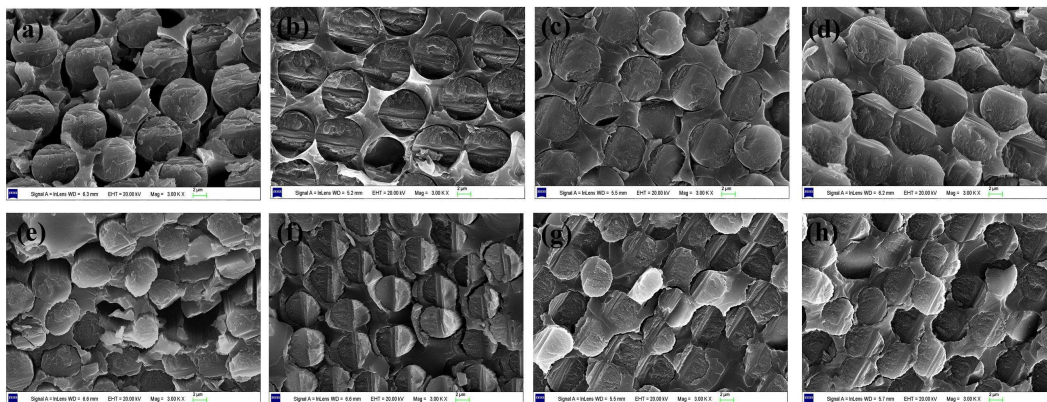


Figure 5

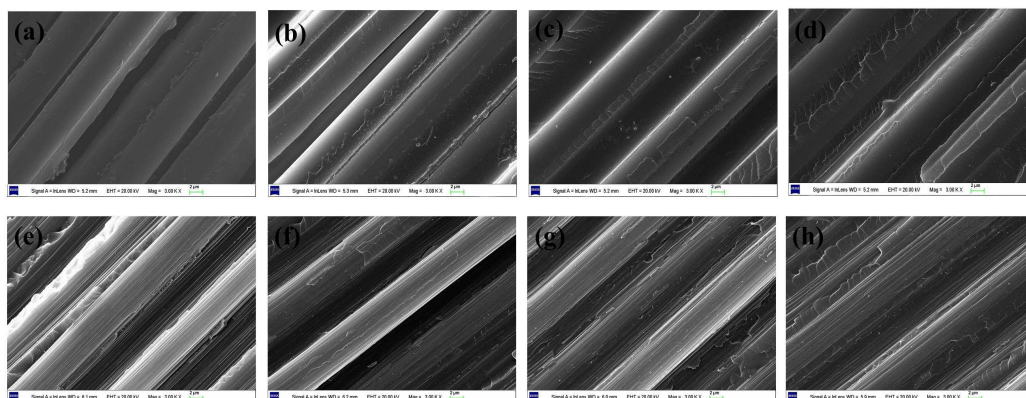


Figure 6

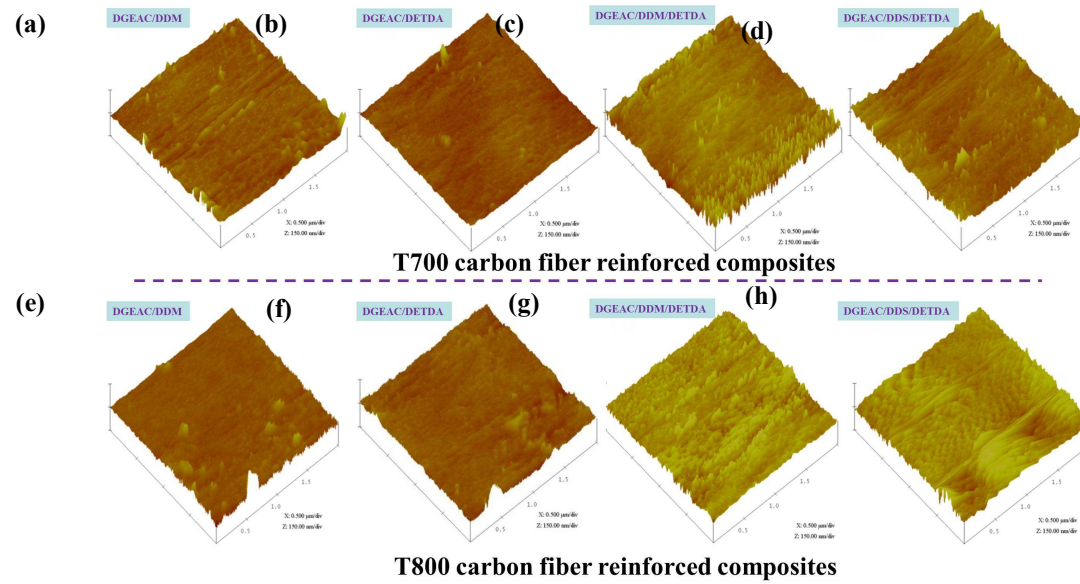


Figure 7

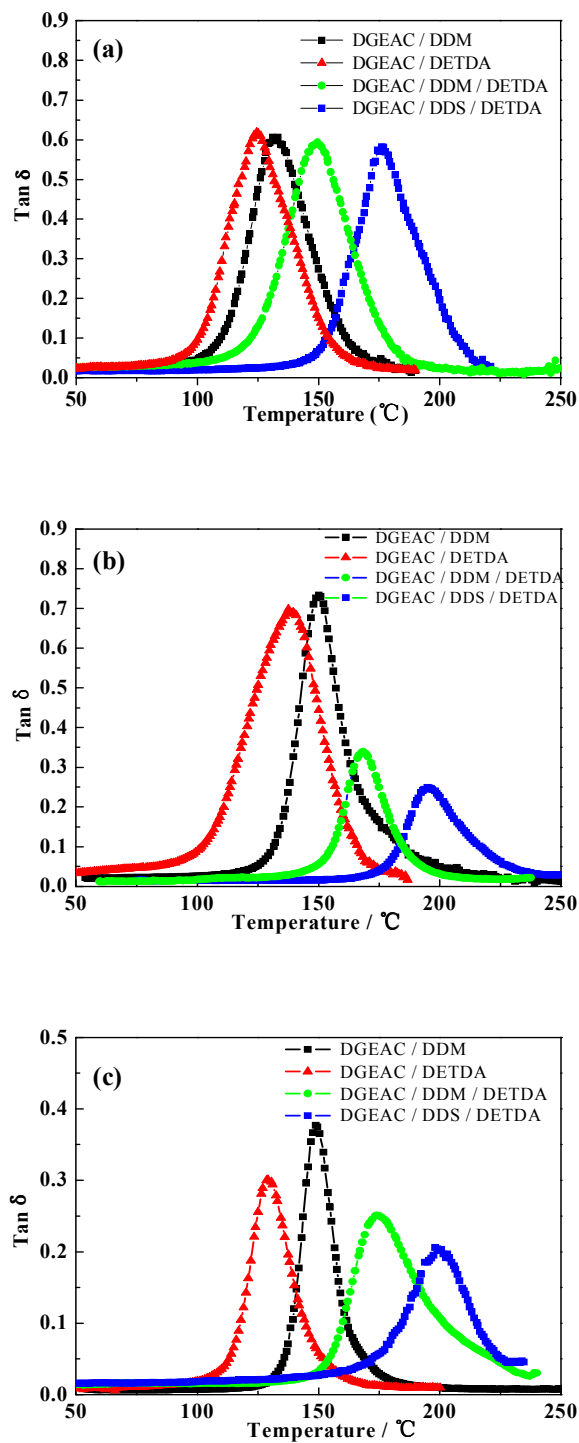


Figure 8

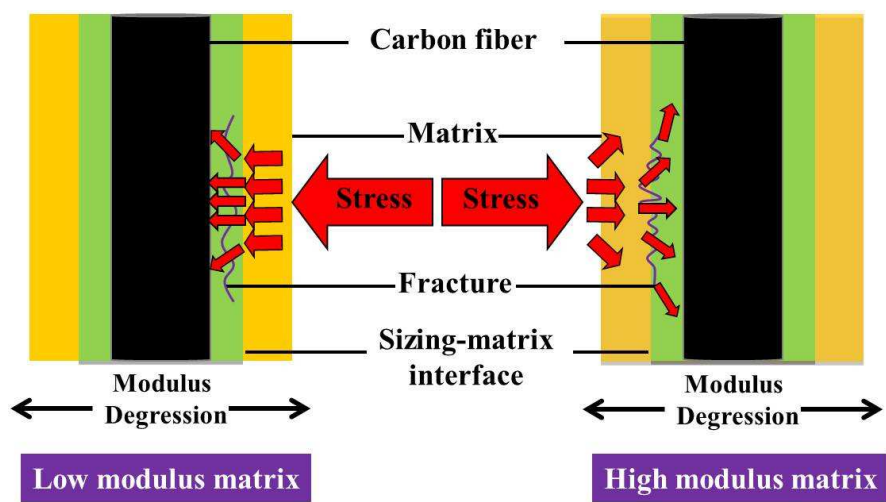


Table 1 Chemical structure of materials

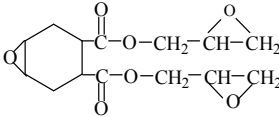
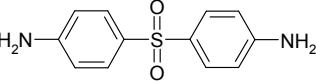
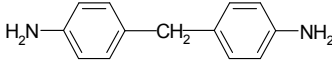
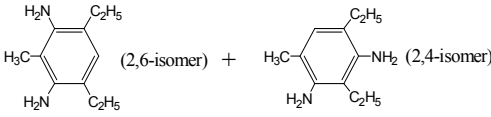
Materials	Chemical structures
DGEAC	
DDS	
DDM	
DETDA	

Table 2 Properties of the T700 carbon fiber and T800 carbon fiber

Carbon fiber	Diameter of single filament (μm)	Tensile strength (GPa)	Tensile modulus (GPa)	Elongation (%)
T700S-12k-50C	7	4.9	230	2.10
T800H-12k-50B	5	5.5	294	1.90

Table 3 Mechanical properties of resin casts

Resin/Hardener	Tensile strength (MPa)	Elongation (%)	Tensile modulus (GPa)
DGEAC/DDM	90±4	4.3±0.2	2.4±0.3
DGEAC/DETDA	81±6	2.6±0.2	3.0±0.2
DGEAC/DDM/DETDA	98±5	4.4±0.2	3.0±0.2
DGEAC/DDS/DETDA	93±3	4.1±0.2	3.7±0.2

Table 4 Mechanical properties of composites

Epoxy/hardener	T700 carbon fiber		T800 carbon fiber	
	NOL ring Tensile strength / MPa	ILSS/MPa	NOL ring Tensile strength / MPa	ILSS/MPa
DGEAC/DDM	1950±203	65±3	2140±304	91±2
DGEAC/DETDA	2130±320	68±2	2410±277	98±3
DGEAC/DDM/DETDA	2200±381	70±1	2530±275	104±2
DGEAC/DDS/DETDA	2380±293	71±3	2680±313	106±2

Table 5 Main roughness parameters of carbon fiber in composites after failure by AFM

Epoxy/hardener	T700 carbon fiber		T800 carbon fiber	
	R _a (nm)	R _{max} (nm)	R _a (nm)	R _{max} (nm)
DGEAC/DDM	22.33	81.89	31.25	125.20
DGEAC/DETDA	32.51	117.63	39.97	167.87
DGEAC/DDM/DETDA	34.45	128.32	42.49	188.30
DGEAC/DDS/DETDA	37.64	136.83	46.77	217.26

Table 6 Interfacial adhesion parameters of T700 and T800 carbon fiber/epoxy composites

Epoxy/hardener	T700 carbon fiber				T800 carbon fiber			
	$(\tan\delta_{\max})_c$	$(\tan\delta_{\max})_m$	A	α	$(\tan\delta_{\max})_c$	$(\tan\delta_{\max})_m$	A	α
DGEAC/DDM	0.739	0.612	2.019	-0.212	0.380	0.612	0.552	0.387
DGEAC/DETDA	0.700	0.625	1.800	-0.125	0.307	0.625	0.228	0.530
DGEAC/DDM/DETDA	0.348	0.602	0.445	0.423	0.255	0.602	0.059	0.578
DGEAC/DDS/DETDA	0.253	0.588	0.076	0.558	0.207	0.588	-0.120	0.635